

Evidence for an Intermediate Mass Black Hole in NGC 5408 X-1

Tod E. Strohmayer¹ & Richard F. Mushotzky¹

ABSTRACT

We report the discovery with XMM-Newton of correlated spectral and timing behavior in the ultraluminous X-ray source (ULX) NGC 5408 X-1. An ≈ 100 ksec pointing with XMM/Newton obtained in January, 2008 reveals a strong 10 mHz QPO in the > 1 keV flux, as well as flat-topped, band limited noise breaking to a power law. The energy spectrum is again dominated by two components, a 0.16 keV thermal disk and a power-law with an index of ≈ 2.5 . These new measurements, combined with results from our previous January 2006 pointing in which we first detected QPOs, show for the first time in a ULX a pattern of spectral and temporal correlations strongly analogous to that seen in Galactic black hole sources, but at much higher X-ray luminosity and longer characteristic time-scales. We find that the QPO frequency is proportional to the inferred disk flux, while the QPO and broad-band noise amplitude (root mean squared, rms) are inversely proportional to the disk flux. Assuming that QPO frequency scales inversely with black hole mass at a given power-law spectral index we derive mass estimates using the observed QPO frequency - spectral index relations from five stellar-mass black hole systems with dynamical mass constraints. The results from all sources are consistent with a mass range for NGC 5408 X-1 from 1000 - 9000 M_{\odot} . We argue that these are conservative limits, and a more likely range is from 2000 - 5000 M_{\odot} . Moreover, the recent relation from Gierlinski et al. that relates black hole mass to the strength of variability at high frequencies (above the break in the power spectrum) is also indicative of such a high mass for NGC 5408 X-1. Importantly, none of the above estimates appears consistent with a black hole mass less than $\approx 1000 M_{\odot}$ for NGC 5408 X-1. We argue that these new findings strongly support the conclusion that NGC 5408 X-1 harbors an intermediate mass black hole.

Subject headings: black hole physics - galaxies: individual: NGC 5408 - stars: oscillations - X-rays: stars - X-rays: galaxies

¹Astrophysics Science Division, NASA's Goddard Space Flight Center, Greenbelt, MD 20771 email: tod.strohmayer, richard.mushotzky@nasa.gov

1. Introduction

The nature of the bright X-ray sources found in nearby galaxies, the ultraluminous X-ray sources (ULXs), remains a major astrophysical puzzle. The fundamental conundrum is that some of these objects have X-ray luminosities uncomfortably high to be stellar-mass black holes (BH) without violating standard Eddington limit arguments. Three different solutions have been proposed for the luminosity problem. 1) The objects are intermediate-mass BHs (Colbert & Mushotzky 1999). 2) They are stellar-mass BHs with, in some cases, substantial beaming of their X-ray radiation (King et al. 2001), or, 3) they are stellar-mass BHs emitting above their Eddington limit (Begelman 2006). It is possible that some ULXs appear ultraluminous because of a combination of all three factors (moderately higher mass, mild beaming and mild super-Eddington emission). It may also be that these objects make up an inhomogeneous population, comprised of both a sub-sample of intermediate-mass BHs and moderately beamed stellar BHs (for recent reviews see Fabbiano & White 2006; Miller & Colbert 2004). Due to their extragalactic nature the study of ULX counterparts at other wavebands has been difficult, and has so far precluded the use of the familiar methods of dynamical astronomy to weigh them. However, recent work has resulted in mass measurements for some Local Group stellar BHs, including IC 10 X-1 (Prestwich et al. 2007; Silverman & Filippenko 2008), and M33 X-7 (Orosz et al. 2007; Liu et al. 2008), but these are not ULXs.

A substantial body of work now supports the idea that timing properties can be used to constrain the masses of BHs. For example, McHardy et al. (2006) have shown that when luminosity variations are taken into account, both stellar-mass and supermassive BHs populate a “variability plane” linking their broad band variability time-scales, luminosities and masses (see also K rding et al. 2007). Casella et al (2008) applied this relation in order to estimate the masses of two ULXs, M82 X-1 and NGC 5408 X-1, concluding that the masses of NGC 5408 X-1, and M82 X-1 lie in the range (in solar units) $115 < M_{bh} < 1300$, and $95 < M_{bh} < 1260$, respectively. However, in this case the scaling was not direct in that Casella et al. (2008) had to estimate the relevant break time-scale from the observed QPO frequencies in M82 X-1 and NGC 5408 X-1. They did this by applying a scaling relation between the two quantities derived only from observations of stellar-mass BHs.

Recently, Gierlinski, Nikolajuk & Czerny (2008) have shown that the strength of high frequency variability—parameterized as the root mean squared (rms) amplitude integrated above the break in the power spectrum—scales approximately linearly with BH mass. They show that a broad correlation exists when comparing stellar and supermassive BHs, but the relation is not tight enough to predict the mass of a stellar system by comparison, for example, with another stellar-mass BH of known mass.

It is now firmly established that Galactic BHs accreting at high rates—often classified as the Intermediate State (IS) or Steep Power-Law state (SPL)—show strong correlations between their spectral and temporal parameters. In these states a significant fraction of the X-ray luminosity is in a power-law component whose spectral index correlates well with the frequency of a QPO (so-called Type C QPOs) that is also commonly detected in such states (see Sobczak et al. 2000; Vignarca et al. 2003; Kalemci et al. 2005; Remillard et al. 2002; Casella et al. 2004). Other spectral parameters also correlate with QPO frequency, such as the disk flux. Recent work by Shaposhnikov & Titarchuk (2007; 2009; hereafter ST07 and ST09) has demonstrated rather convincingly that the QPO frequency - spectral index scaling for Type C QPOs can be used as an empirical BH mass estimator. Previous efforts have been made to use this scaling argument to constrain the masses of ULXs (Fiorito & Titarchuk 2004; Dewangan, Titarchuk & Griffiths 2006; Strohmayer et al. 2007, hereafter Paper 1), however, in these previous studies, there was no direct evidence to indicate that the QPO properties seen in the ULX sources actually correlates with the spectral parameters as in stellar-mass systems.

In this paper we present the results of new timing and spectral measurements that show for the first time that NGC 5408 X-1 behaves very much like a Galactic stellar-mass BH system with the exception that its characteristic X-ray time-scales are ~ 100 times longer, and its luminosity is greater by a roughly similar factor. We argue that these new findings provide strong evidence that this system contains a few thousand solar mass BH.

2. New XMM-Newton Observations and Data Analysis

Paper 1 summarizes results from XMM-Newton observations obtained in 2006 January in which X-ray QPOs were detected from NGC 5408 X-1 for the first time (we sometimes also refer to this as Observation 1). In order to look for correlated timing and spectral behavior we sought and obtained additional XMM-Newton observations in 2008 January. These new observations began on January 13, 2008, and continued for ≈ 116 ksec (Observation 2). We used the standard SAS version 8.0.0 tools to filter and extract images and event tables for both the pn and MOS cameras. We extracted events in an $18''$ radius around the source in both the pn and MOS cameras. Due to its higher count rate and better time resolution we began our timing study using the pn data.

2.1. Power Spectral Timing Analysis

There was some background flaring present during our observation which broke up the exposure into several useful intervals. We work with the four longest intervals, labeled A through D in time order, and with exposures of 15.9, 23.0, 20.0 and 13.6 ksec, respectively. Figure 1 shows the pn lightcurve in 78 s bins for the longest interval (interval B).

We began our timing analysis by making average power spectra by combining all good intervals. Based on the energy dependent variability behavior exhibited in observation 1 (see Paper 1) we made power spectra in several energy bands; 0.2 - 8 keV, 1 - 8 keV, and 2 - 8 keV. We found a prominent peak at 10 mHz in the 1 - 8 keV power spectrum. Figure 2 shows the average power spectrum binned at 0.64 mHz in which we found the peak. To assess the significance of the peak we first rescaled the power spectrum. We did this by fitting a bending power-law continuum to the spectrum, excluding the two highest bins in the peak to avoid biasing the fit to higher values. We then divided the power spectrum by the best-fitting continuum model. This procedure is important when searching for QPOs against an intrinsic, broad-band noise component as is present in NGC 5408 X-1. We estimate the significance as the chance probability of obtaining the highest observed peak in the rescaled power spectrum using for the noise power distribution the χ^2 distribution with 176 degrees of freedom (dof). This is the expected distribution given the number of independent frequency bins that were averaged (88). We compared the distribution of powers in our observed power spectrum with this expected distribution and confirmed they are consistent. This then gives a chance probability, per trial, of 3.7×10^{-8} . We searched out to 0.5 Hz and this was the 2nd power spectrum searched, giving a total of $390 \times 2 = 780$ independent trials, resulting in a significance of 2.9×10^{-5} , a strong detection.

To further quantify the variability we fit the same continuum model but now including a Lorentzian to account for the QPO. This model fits well, with a best fitting $\chi^2 = 463$ for 459 degrees of freedom, and is shown in Figure 2. Removing the QPO component from the fit results in an increase in χ^2 of 49. For the addition of three additional QPO parameters, this increase in χ^2 gives a chance probability by the F-test of 5×10^{-10} , further supporting the detection.

The QPO has a centroid frequency of 10.24 ± 0.005 mHz, and a coherence of $\nu_{cent} / \Delta\nu_{fwhm} \approx 20$. The QPO is strong, with an average amplitude (rms) in the > 1 keV band of $17.4 \pm 1.3\%$. We do not detect the QPO at energies below 1 keV, with a 90% upper limit on the amplitude (rms) of 4.5%, demonstrating that the amplitude of the QPO is a strong function of energy. The band-limited noise is also quite strong, with an integrated amplitude (rms) of $41 \pm 5\%$ (1 - 100 mHz). Similarly to the QPO the broad-band noise amplitude is also stronger at higher energies. This behavior is typical of Galactic BHs as well (Nowak et al. 1999; Belloni

et al. 2005).

We next examined the intervals separately. For the longest interval (B) we again detect the 10 mHz QPO, but we also find evidence for a second QPO at 13.4 mHz. Figure 3 (upper curve) shows the power spectrum from interval B in the 1–8 keV energy band. The 13.4 mHz feature is significant at a bit better than the 3σ level, so we consider it robust. Interestingly, these two peaks have frequencies consistent with a ratio of 4:3. A pair of QPOs with a similar frequency ratio were also detected in observation 1 (see paper 1). These similarities provide added confidence that the 13.4 mHz QPO is significant. Combining the two longest intervals (B and C) above 1 keV gives a power spectrum with a strong detection of the 10 mHz feature, as well as two other candidate features (see Figure 3, lower curve). The higher frequency QPO at 13.4 mHz is still present, though it is less prominent than in interval B alone, and a third feature is suggested at 6 mHz. We modeled this power spectrum with the same bending power-law continuum and included up to three QPO components. We find a statistically acceptable fit with $\chi^2 = 518.8$ (497 degrees of freedom). The 10 mHz QPO is absolutely required, as removing it from the fit increases χ^2 by 96, better than an 8σ detection based on the F-test. Removing the lowest and highest frequency QPO components one at a time results in increases in χ^2 of 17.7 and 29.2, respectively. These correspond to F-test probabilities of 2.6×10^{-4} and 6.9×10^{-7} , respectively, for the additional components. While this provides rather strong evidence for the 13.4 mHz QPO, we regard the 6 mHz feature as tentatively detected.

In summary, our new observations of NGC 5408 X-1 reveal a strong QPO at 10 mHz, and very strong “flat-topped” band-limited noise breaking to a power law, with the break close to the QPO. This behavior is qualitatively similar to results from our 2006 observations, but with the QPO and break frequencies shifted down in frequency by about a factor of two, and with stronger rms variability.

2.2. Energy Spectral Analysis

Previous spectral studies have shown that NGC 5408 X-1 has a cool thermal disk component with $kT \approx 0.15$ keV and a power-law extending to higher energies with a slope of ≈ 2.5 (Kaaret et al. 2003; Soria et al. 2004; Paper 1). We obtained a pn spectrum by extracting an 18” region around the source. Background was obtained from a nearby circular region free of sources. We began by fitting the present spectrum with the same model components used to describe our 2006 data (paper 1); a relativistic disk (*diskpn* in XSPEC), a power-law, and a thermal plasma (*apec* in XSPEC). These were modified by successive photoelectric absorption components, one fixed at the best Galactic value ($n_H = 5.7 \times 10^{20}$

cm^{-2}), the other left free to account for possible local absorption. This model provides an acceptable fit, and from a qualitative standpoint the spectral parameters are similar to those derived from our 2006 observations. The disk temperature of 0.16 ± 0.005 keV is consistent within the errors to that derived from the 2006 data. The power-law index, at 2.47 ± 0.04 , is slightly smaller than the previous measurement, but only different at about the 2σ level. We searched for line emission in the Fe band but did not detect any significant features. However, the limits are not that constraining, with an 90% confidence upper limit on the equivalent width at 6.4 keV of ≈ 350 eV.

The thermal plasma model parameters and flux are consistent with the 2006 data, contributing a 0.3 - 10 keV flux of $\approx 1 \times 10^{-13}$ erg cm^{-2} s^{-1} in each observation. Examination of *Chandra* images of NGC 5408 indicate the existence of extended emission co-spatial with NGC 5408 X-1. This emission is unresolved in the XMM observations of NGC 5408 X-1, and we suggest that this spectral component is likely associated with star formation in NGC 5408 and not intrinsic to the ULX. We will compare and contrast the spectral results from the two epochs in more detail below.

3. Comparison of 2006 and 2008 Observations: Timing - Spectral Correlations

We can now compare the timing and spectral properties from the two epochs, and determine whether or not NGC 5408 X-1 shows patterns of behavior similar to that seen in Galactic BHs. We begin with a more detailed comparison of the energy spectrum and fluxes during the two observations. For consistency we re-extracted the spectrum from the 2006 observations to include essentially all of the good exposure, and in each epoch the spectrum represents the total accumulated over the entire observation. We produced count rate spectra for each observation and Figure 4 shows the difference spectrum as a function of energy (Observation 1 - Observation 2). One can see from the figure that the first observation (2006) had a higher count rate, and that most of the difference is in the < 1 keV band, which is dominated by the disk flux. This demonstrates that the 2006 observation had relatively more counts in the soft band (< 1 keV), and less in the power-law component extending to higher energy. Table 2 provides a detailed comparison of the spectral parameters derived from the two epochs. The unabsorbed flux (0.3 - 10 keV) in 2008 was 3.1×10^{-12} , about 12% less than the 2006 observation, and the power-law component represents a greater fraction of the total flux than in the 2006 data. The two most important conclusions are that the disk flux was about 20% higher in Observation 1, and that the power-law component contributes a greater fraction of the total flux in Observation 2.

We next compared power spectra accumulated during each observation. Figure 5 shows

power spectra characteristic of each epoch. The upper curve is data from our 2008 observations, and the lower curve is from 2006 (see also Paper 1, Figure 3). These power spectra were not accumulated over the exact same energy bands. Because the variability has a significant energy dependence, and because a primary goal is to compare the characteristic time-scales in each epoch, we choose to compare the spectra in the energy bands where the signal to noise ratio of the respective QPOs is largest. For the 2006 data this corresponds to 0.2 - 8 keV, whereas for the 2008 data we use, of the bands searched, the 1 - 8 keV band. Table 1 compares relevant timing properties for the two observations. Timing properties were derived from the model fits shown in Figure 5 using the bending power-law continuum and Lorentzian components for the QPOs. We note that the bend frequency in the 0.2 – 8 keV 2006 data we used to compare the 2006 and 2008 QPO parameters is not well constrained. A more representative value is the bend frequency of ≈ 25 mHz derived from the > 2 keV 2006 data (Paper 1). In general, the measurement of the QPO frequency in both epochs is much more precise than the bend frequency, which is why we emphasize it in our comparisons of the two epochs.

Closer examination of Figure 5 reveals several important conclusions concerning the variability in NGC 5408 X-1. We see that the strongest QPO has shifted from 20 to 10 mHz, over the same time that the disk flux dropped by 20%. Additionally, the photon power-law index decreased modestly as the QPO frequency dropped. These behaviors are entirely consistent with what has been observed in Galactic BHs with so-called Type C QPOs (see, for example, Sobczak et al. 2000; Vignarca et al. 2003; Kalemci et al. 2005).

Another strikingly evident feature in Figure 5 is the larger amplitude of the variability (broad-band and QPO) in the 2008 observation (top). This quantity is proportional to the integral of the power spectrum above the poisson level (here a value of 2), which is clearly larger in the 2008 observations. The rms amplitude also has a scaling with the square root of the count rate, but this was smaller in the 2008 observations, so this effect simply makes the apparent difference larger. We also compared the rms amplitudes *in the same energy band*, and the conclusion is unchanged. Again, the higher rms variability at the epoch of lower disk flux is strikingly similar to what is observed in Galactic systems. Here the primary conclusion is that the variability is mostly carried by the power-law component, and not the disk flux. So, when the power-law becomes more dominant, then the rms amplitude increases. Finally, we note that the modest drop in the power-law index with the decrease in QPO frequency is also consistent with the correlations seen in Galactic systems. In this case the relatively small change in the index accompanying a larger change in QPO frequency suggests that the power-law index in NGC 5408 X-1 may be near “saturation” of the scaling (see for example, Figure 5 in Vignarca et al. 2003; ST09), that is, both the QPO frequency and index are near their upper ranges in the correlation. This conclusion is also supported

by the behavior of the rms amplitude. The strong drop in the rms amplitude at relatively constant power-law index is consistent with the QPO frequency being at the higher end of the observed correlations (see, for example, the behavior of XTE J1550-564 illustrated in Figure 5a from Sobczak et al. 2000).

4. Discussion and Implications

Our new observations of NGC 5408 X-1 reveal correlated variations in its timing and spectral properties very much like a stellar-mass black hole. Indeed, the evidence is now quite compelling that the strong low frequency QPO detected on several occasions from NGC 5408 X-1 is a Type-C QPO analogous to those seen in Galactic systems. It varies in frequency and amplitude with changes in flux and spectrum in a manner entirely consistent with the behavior in Galactic BHs such as XTE J1550-564 and GRS 1915+105. Whereas these stellar-mass systems have characteristic QPO frequencies of a few Hz, NGC 5408 X-1 shows QPO frequencies lower by a factor ~ 100 while simultaneously radiating an X-ray luminosity larger by a roughly similar factor.

Given greater confidence in the identification of and scaling properties of the strong QPO seen in NGC 5408 X-1 we can use it to derive a mass estimate. We essentially follow the scheme outlined by ST09. We use the QPO frequency - power-law index correlations measured for five systems; GRS 1915+105 (Vignarca et al. 2003), XTE J1550-564, XTE J1859+226, H 1743-322 and GX 339-4 (ST09). We use these systems as our primary sources for mass estimates because they have both measured power-law indices that overlap the range of observed indices in NGC 5408 X-1, and reasonable BH mass estimates from dynamical measurements.

Since we do not yet have a correlation from NGC 5408 X-1 with many points to scale from we carry out a simplified procedure. For our reference Galactic systems we find the range of QPO frequencies with power-law indices between 2.4 and 2.6. We choose this index range as representative and conservative. It is 2σ below the lower best fit value (from 2008) and 2σ above the higher best-fit value (from 2006) for NGC 5408 X-1. In the case that a range of QPO frequency exists at either end of our index range, we take the largest range of observed frequencies. To be specific, we take the lowest frequency measured at an index of 2.4, and the highest frequency found at an index of 2.6. We then find the multiplicative scale factor, f , required to bring the lower and upper QPO values measured for NGC 5408 X-1 (10 and 20 mHz) into agreement with the measured frequency range for our reference systems. In the case that a constant scale factor cannot match both the lower and higher frequencies of the observed range, we find the scale factor that aligns the centers of the two

ranges (we call this estimate f_{best}). The derived mass estimate for NGC 5408 X-1 is then the mass of the reference stellar system times the scale factor. In one case, H 1743-322, frequency measurements exist only near the low end of our target index range (2.4). In this case we derive the scale factor by simply scaling to the lower QPO frequency measured in NGC 5408 X-1. The derived scale factors and mass estimates based on comparison with these five reference systems are summarized in Table 3.

The quoted uncertainty on the best mass estimate in Table 3 reflects the uncertainty in the masses of the reference systems (where available), that is, assuming a “correct” scale factor. The QPO frequency and power-law index measurements for NGC 5408 X-1 described here are rather precise, so that if all the assumptions made with regard to the mass scaling arguments above are accurate, then the amount of statistical error in the estimates is modest. This leaves systematic uncertainties, that is, how accurate is the derived scale factor? Now, some Galactic BHs do show variations in their QPO frequency – spectral index correlations. These are primarily associated with apparent changes in the value of the spectral index at which the correlation saturates (see, for example, the behavior of XTE J1550-564 in Figure 7 from ST09), or simply that the correlation is not exact, and that at a given index value, there can be a range of measured QPO frequencies. We took into account such variations in defining the range of QPO frequencies to scale to for each reference system. However, the existence of a range of measured frequencies at a given spectral index suggests a conservative way to bound the scale factor systematic error, by defining a minimum and maximum scale factor given the observed QPO frequency range. We do this by scaling the lowest observed QPO frequency in our reference systems with the highest observed QPO frequency in NGC 5408 X-1, and vice versa. For example, for XTE J1550-564, which has observed QPO frequencies from 2.5 - 6.5 Hz, the minimum and maximum scale factors would be (2.5 Hz) / (0.02 Hz) = 125, and (6.5 Hz) / (0.01 Hz) = 650. Based on these limits on the scale factor we also derive minimum and maximum mass estimates by multiplying the maximum and minimum scale factors by the $\pm 1\sigma$ mass limits for each reference system. Both the scale factor ranges and minimum and maximum mass estimates are also given in Table 3. We emphasize that we think these represent rather conservative limits.

While the derived mass ranges in Table 3 are rather large—and we emphasize that this is not a precision mass measurement technique—there is substantial overlap among the estimates from all the different sources. Perhaps more interesting is that all the scaling estimates suggest a BH with a mass comfortably greater than $1000M_{\odot}$, that is, much greater than the current known mass range for stellar BHs. We note that the candidate BH system 4U 1630-47—which is not a dynamically confirmed BH—also has QPO frequency measurements that overlap our target range of spectral index (see Figure 9 in Vignarca et al. 2003). In this source the frequency range is $\approx 4 - 8$ Hz, suggesting a best scale factor of 400, which

falls in the range derived for our other reference systems. While it's mass is not known, a typical value of $\sim 10 M_{\odot}$ would also suggest a mass for NGC 5408 X-1 in the range of several thousand M_{\odot} , consistent with the other sources.

4.1. Other Concerns and Caveats

One concern with regard to QPO frequency scaling arguments has been which QPO frequency to scale to. For example, both XTE J1550-564 and GRS 1915+105 can sometimes show QPO frequencies below 1 Hz, approaching 0.1 Hz in the case of XTE J1550-564. However, our observations of QPOs from NGC 5408 X-1 at different epochs, and with different frequencies and rms amplitudes goes along way towards alleviating this concern. In fact, the behavior of the QPO rms amplitude in NGC 5408 X-1 is completely reversed to what one would expect for a scaling with the lowest QPO frequencies observed in XTE J1550-564 and GRS 1915+105. Results from XTE J1550-564 show that at low QPO frequency, the rms increases with an increase in QPO frequency (see Figure 5a in Sobczak et al. 2000), but this is exactly opposite to the behavior seen in NGC 5408 X-1. The behavior of the QPOs in both XTE J1550-564 and GRS 1915+105 when the power-law index and frequency are both high is a much better match to the behavior seen in NGC 5408 X-1.

Another concern has been that while QPO frequency scalings may give one result, a simple scaling of luminosities gives another, and that the two may not be in agreement. Here one must try to be consistent and compare luminosities under the same conditions. In the case of our scaling arguments this would be to match luminosities at the appropriate power-law index and scaled QPO frequency. An important issue here is that in many cases the distances to BHs in the Galaxy are relatively less well known than the distances to nearby galaxies hosting ULXs. Nevertheless, we can attempt to compare the luminosity of NGC 5408 X-1 to some of our reference BHs. For XTE 1550-564, ST09 report X-ray spectral and QPO frequency measurements. For power-law index and QPO frequency appropriate to our scaling the observed X-ray flux from XTE J1550-564 (2 - 20 keV) was in the range $3 - 5 \times 10^{-8} \text{ erg cm}^{-2} \text{ s}^{-1}$. The distance to this source is not very well constrained, with estimates ranging from 2.5 - 6 kpc. Taking a flux of $4 \times 10^{-8} \text{ erg cm}^{-2} \text{ s}^{-1}$ as representative, we have a luminosity of $5 \times 10^{37} (d/3\text{kpc})^2$. This compares with a representative luminosity from our 2006 observation of about $1.1 \times 10^{40} \text{ erg cm}^{-2} \text{ s}^{-1}$ (0.2 - 10 keV; assuming a distance of 4.8 Mpc). The luminosity ratio is then in the range of 317 - 55, for the distance range of 2.5 - 6 kpc for XTE J1550-564. Simply scaling up the $\pm 1\sigma$ mass range for XTE J1550-564 by these limits gives a mass estimate for NGC 5408 X-1 of 462 – 3360 M_{\odot} . Interestingly, ST09 use an observed correlation in the power-law index and bulk motion comptonization

model normalization (model *bmc* in XSPEC) to estimate distances as well as BH masses by scaling to a reference system. Interestingly, they favor a distance closer to 3 kpc than 6 kpc for XTE J1550-564, which would favor the high end of the derived mass range. For GRS 1915+105, again the distance is rather uncertain, likely being in the range from 6 – 12 kpc (Dhawan et al. 2007). For the QPO frequency range above a representative flux range is about $2 - 5 \times 10^{-8}$ erg cm⁻² s⁻¹ (Muno et al. 1999), giving a range of luminosity ratio of 73 – 18.2. Similar scaling as for XTE J1550-564 would imply a mass range from 182 – 1314 M_{\odot} . While this range appears systematically smaller than the mass range inferred from the QPO scaling, it still overlaps with the minimum mass estimate for GRS 1915+105.

4.2. Amplitude of High Frequency Variability

Recently, Gierlinski et al. (2008) have argued that the amplitude of X-ray variability at high frequencies can be used as an estimator of BH mass. Their hypothesis is that there is a “universal” power spectral shape for BHs at high frequency. Here, high frequency means above the break in the power spectrum. This universal form is roughly a power law with index of 1.5 - 2.0. They explore the notion that this part of the power spectrum is nearly constant for a given source, but scales with BH mass. They find that there is a roughly linear correlation extending from the stellar-mass BHs to AGN (using type 1 Seyferts). The relation is not exact, and the scatter is such to make it difficult to estimate the mass of a stellar BH by scaling from another stellar-mass system, however, for order of magnitude estimates the method seems reasonably robust. We used our power spectrum continuum models (above the bend or break in the spectrum) to estimate the parameter C_M , which is simply the normalization of the high frequency power-law component at 1 Hz. We integrated our best fitting continuum models from the bend frequency to 0.5 Hz in order to estimate C_M (see Eqn. 2 in Gierlinski et al. 2008). We find $\pm 1\sigma$ ranges of $-3.23 < \log C_M < -3.13$, and $-3.66 < \log C_M < -3.55$ for the 2008 and 2006 observations, respectively. These values correspond to mass ranges of 1686 - 2612, and 4435 - 5714 M_{\odot} , respectively, for the best fitting correlation derived by Gierlinski et al., and 3737 - 4704, and 9828 - 12661 M_{\odot} using their soft-state relation derived from Cyg X-1. While the possible mass range from this method is large, the C_M values for NGC 5408 X-1 fall almost midway between the stellar-mass systems and NGC 4395, a low mass AGN (see Figure 7 in Gierlinski et al. 2008), and comfortably within the mass range consistent with intermediate mass BHs.

5. Summary and Conclusions

Our new XMM-Newton observations have revealed for the first time that NGC 5408 X-1 exhibits correlated X-ray timing and spectral properties quite analogous to those exhibited by Galactic stellar-mass BHs in the “very high” or “steep power-law” state. Its longer observed time-scales (QPO and power spectral break frequencies) at higher luminosity compared to Galactic stellar-mass BHs can be understood if the mass of NGC 5408 X-1 is a few thousand solar masses. We have arrived at this conclusion by several independent arguments. Given our present understanding of the timing properties of BHs at all mass scales, it seems to us hard to escape the conclusion that NGC 5408 X-1 is an intermediate mass BH.

We have again found evidence for a pair of sharp, closely spaced QPOs in NGC 5408 X-1 with a frequency ratio consistent with 4:3. We thus conclude that this is an intrinsic feature of the system and not some artifact or coincidence associated with having only a single observation of the source. As we noted in Paper 1, it is possible that this results from detection of both a Type C QPO (the stronger feature), and a Type B QPO (Casella et al. 2004). If the source transitions from one to another, we do not have sufficient signal to noise ratio data to “watch” such transitions occur. Rather, we simply see average detections of each QPO.

We have argued that the observed variations in QPO frequency, accompanied by spectral changes consistent with behavior seen in Galactic systems, allows the mass of NGC 5408 X-1 to be estimated by scaling the observed QPO frequencies to match those observed in stellar-mass systems of known mass. Essentially the same method has now been used on a good number of Galactic systems and seems empirically robust (ST09). These arguments give mass estimates for NGC 5408 X-1 in a broad range from $1 - 9 \times 10^3 M_{\odot}$, however, we find that none of the QPO scaling estimates are consistent with masses below $\approx 1000 M_{\odot}$. Independent mass constraints based on the amplitude of high frequency variability also appear consistent with this range. Additional observations would help to map out the timing - spectral correlations for NGC 5408 X-1 more clearly, and thus allow more rigorous estimates. As noted in Paper 1, the measured disk temperature in NGC 5408 X-1 is also consistent with a few thousand M_{\odot} BH if the theoretical accretion disk scaling of $kT_{disk} \propto M^{-1/4}$ holds. Importantly, none of these new estimates appears consistent with a mass as low as even a few hundred solar masses. We think these new findings provide strong evidence that NGC 5408 X-1 harbors an intermediate mass BH.

We thank the anonymous referee for a careful review of the manuscript that helped us to improve the paper.

REFERENCES

- Begelman, M. C. 2006, *ApJ*, 643, 1065.
- Belloni, T., Homan, J., Casella, P., van der Klis, M., Nespoli, E., Lewin, W. H. G., Miller, J. M., & Méndez, M. 2005, *A&A*, 440, 207.
- Casella, P., Ponti, G., Patruno, A., Belloni, T., Miniutti, G., & Zampieri, L. 2008, *MNRAS*, 387, 1707.
- Casella, P., Belloni, T., Homan, J., & Stella, L. 2004, *A&A*, 426, 587.
- Colbert, E. J. M. & Mushotzky, R. F. 1999, *ApJ*, 519, 89.
- Dewangan, G. C., Titarchuk, L., & Griffiths, R. E. 2006, *ApJ*, 637, L21.
- Dhawan, V., Mirabel, I. F., Ribó, M., & Rodrigues, I. 2007, *ApJ*, 668, 430.
- Fabbiano, G. & White, N. E. 2006, in “Compact Stellar X-ray Sources,” ed. W. H. G. Lewin, & M. van der Klis, (Cambridge University Press: Cambridge), pg. 475.
- Filippenko, A. V., & Chornock, R. 2001, *IAU Circ.*, 7644, 2.
- Fiorito, R., & Titarchuk, L. 2004, *ApJ*, 614, L113.
- Gierliński, M., Nikolajuk, M., & Czerny, B. 2008, *MNRAS*, 383, 741.
- Greiner, J., Cuby, J. G., & McCaughrean, M. J. 2001, *Nature*, 414, 522.
- R. I. Hynes, D. Steeghs, J. Casares, P. A. Charles, and K. O’Brien 2004 *ApJ* 609, 317.
- Kaaret, P., Corbel, S., Prestwich, A. H., & Zezas, A. 2003, *Science*, 299, 365.
- Kalemci, E., Tomsick, J. A., Buxton, M. M., Rothschild, R. E., Pottschmidt, K., Corbel, S., Brocksopp, C., & Kaaret, P. 2005, *ApJ*, 622, 508.
- King, A. R., Davies, M. B., Ward, M. J., Fabbiano, G. & Elvis, M. 2001, *ApJ*, 552, L109.
- Körding, E. G., Migliari, S., Fender, R., Belloni, T., Knigge, C., & McHardy, I. 2007, *MNRAS*, 380, 301.
- Liu, J., McClintock, J. E., Narayan, R., Davis, S. W., & Orosz, J. A. 2008, *ApJ*, 679, L37.
- McClintock, J. E., Remillard, R. A., Rupen, M. P., Torres, M. A. P., Steeghs, D., Levine, A. M., & Orosz, J. A. 2009, *ApJ*, 698, 1398.

- McHardy, I. M., Koerding, E., Knigge, C., Uttley, P., & Fender, R. P. 2006, *Nature*, 444, 730.
- Miller, M. C., & Colbert, E. J. M. 2004, *International Journal of Modern Physics D*, 13, 1.
- Muno, M. P., Morgan, E. H. & Remillard, R. A. 1999, *ApJ*, 527, 321.
- Muñoz-Darias, T., Casares, J., & Martínez-Pais, I. G. 2008, *MNRAS*, 385, 2205.
- Nowak, M. A., Vaughan, B. A., Wilms, J., Dove, J. B., & Begelman, M. C. 1999, *ApJ*, 510, 874.
- Orosz, J. A., et al. 2007, *Nature*, 449, 872.
- Orosz, J. A., et al. 2002, *ApJ*, 568, 845.
- Prestwich, A. H., et al. 2007, *ApJ*, 669, L21.
- Remillard, R. A., Muno, M. P., McClintock, J. E. & Orosz, J. A. 2002, *ApJ*, 580, 1030.
- Shaposhnikov, N., & Titarchuk, L. 2009, *ApJ*, 699, 453 (ST09).
- Shaposhnikov, N., & Titarchuk, L. 2007, *ApJ*, 663, 445.
- Silverman, J. M., & Filippenko, A. V. 2008, *ApJ*, 678, L17.
- Sobczak, G. J., McClintock, J. E., Remillard, R. A., Cui, W., Levine, A. M., Morgan, E. H., Orosz, J. A., & Bailyn, C. D. 2000, *ApJ*, 531, 537.
- Soria, R., Motch, C., Read, A. M., & Stevens, I. R. 2004, *A&A*, 423, 955.
- Strohmayer, T. E., Mushotzky, R. F., Winter, L., Soria, R., Uttley, P., & Cropper, M. 2007, *ApJ*, 660, 580.
- Uttley, P., & McHardy, I. M. 2005, *MNRAS*, 363, 586.
- Vignarca, F., Migliari, S., Belloni, T., Psaltis, D., & van der Klis, M. 2003, *A&A*, 397, 729.
- Zurita, C., et al. 2002, *MNRAS*, 334, 999.

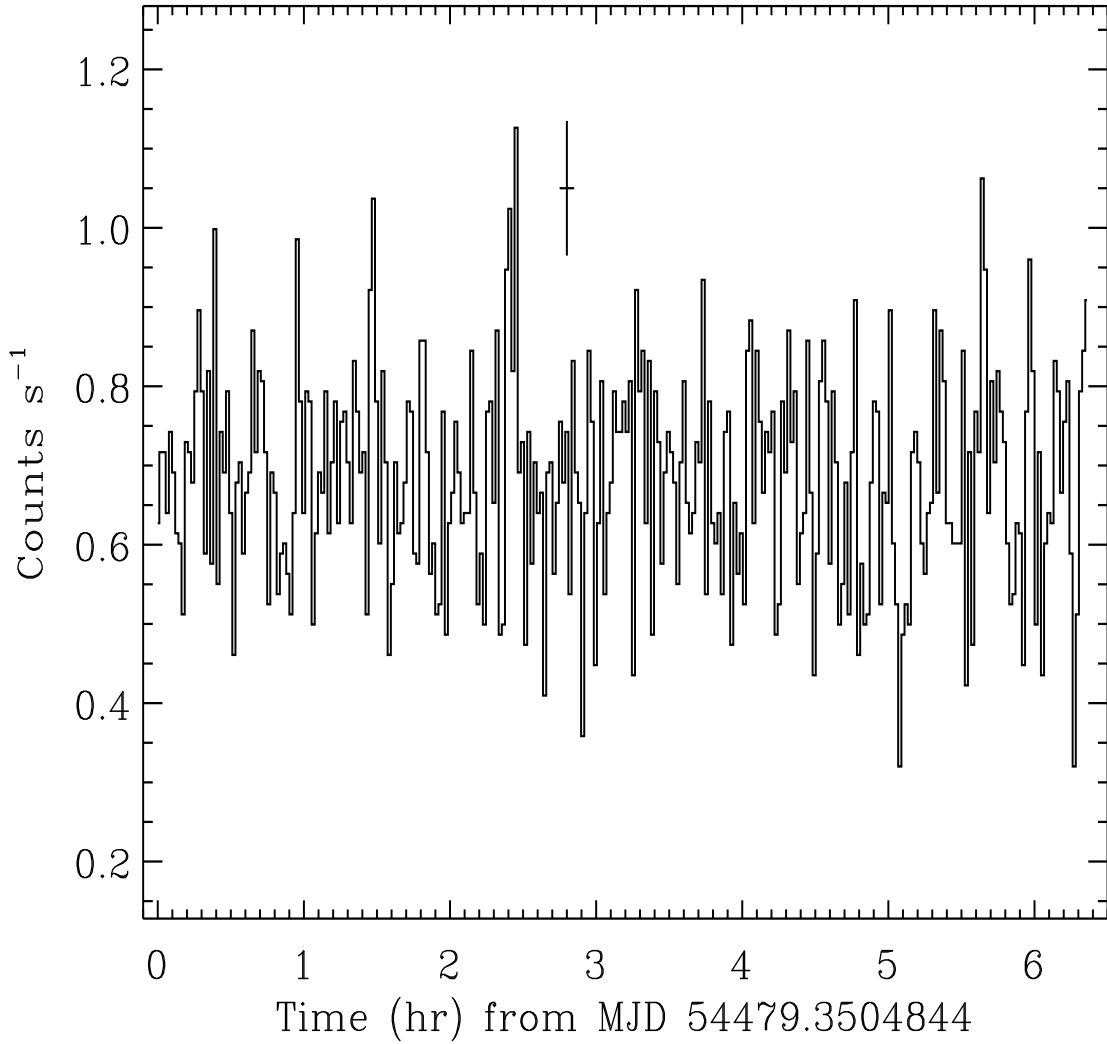


Figure 1: Lightcurve of NGC 5408 X-1 (0.2 - 15 keV band) from XMM-Newton EPIC/pn observations showing the longest contiguous time interval used in our power spectral analysis (Interval B). The bin size is 78.125 seconds. A characteristic error bar is also shown.

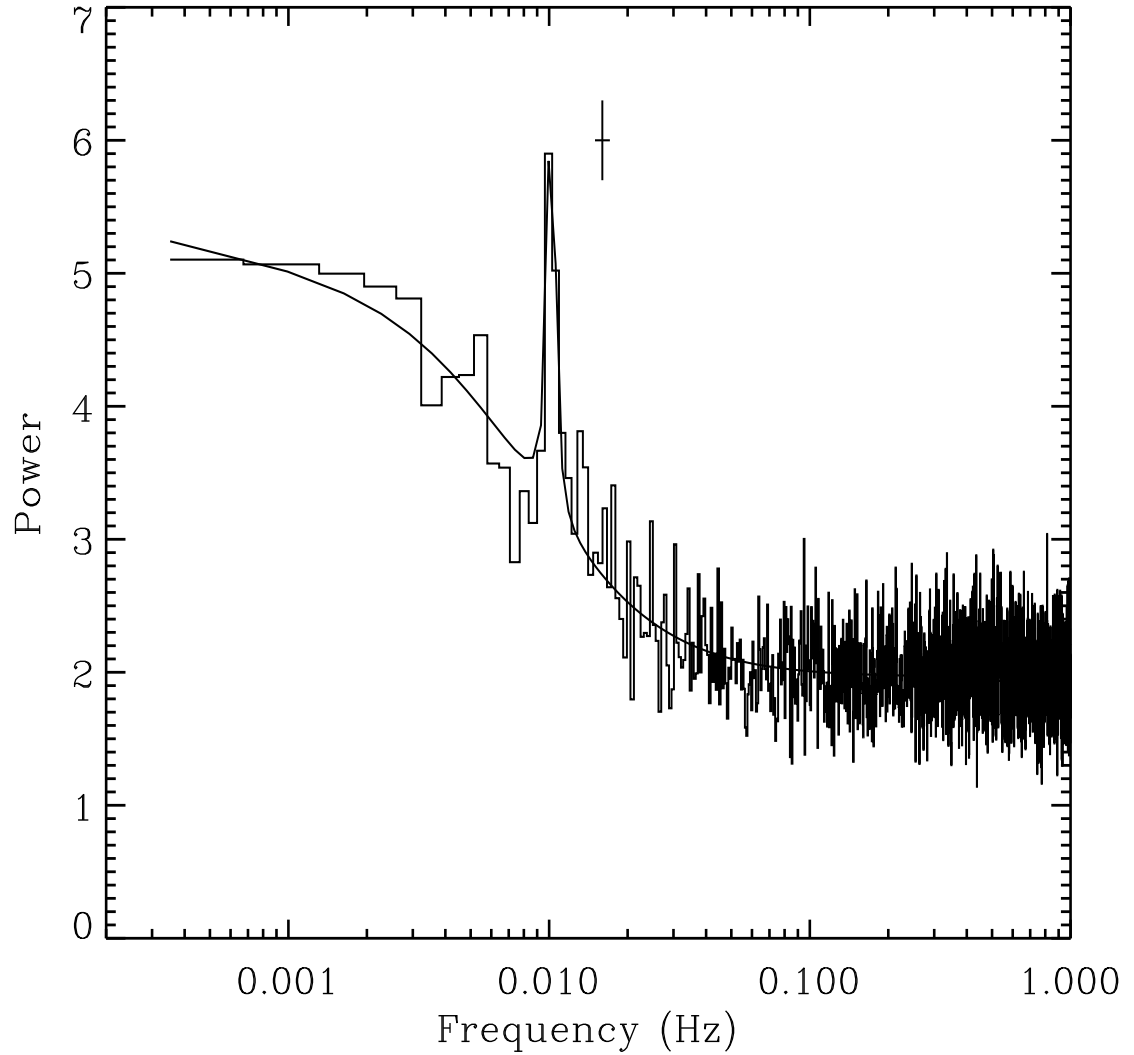


Figure 2: Average power spectrum of NGC 5408 X-1 from the > 1 keV EPIC/pn data (histogram) and the best fitting model (solid). The frequency resolution is 0.64 mHz, and each bin is an average of 44 independent power spectral measurements. The effective exposure is ≈ 70 ksec. A characteristic error bar is also shown. See the text for a detailed discussion of the model, and Table 1 for model parameters.

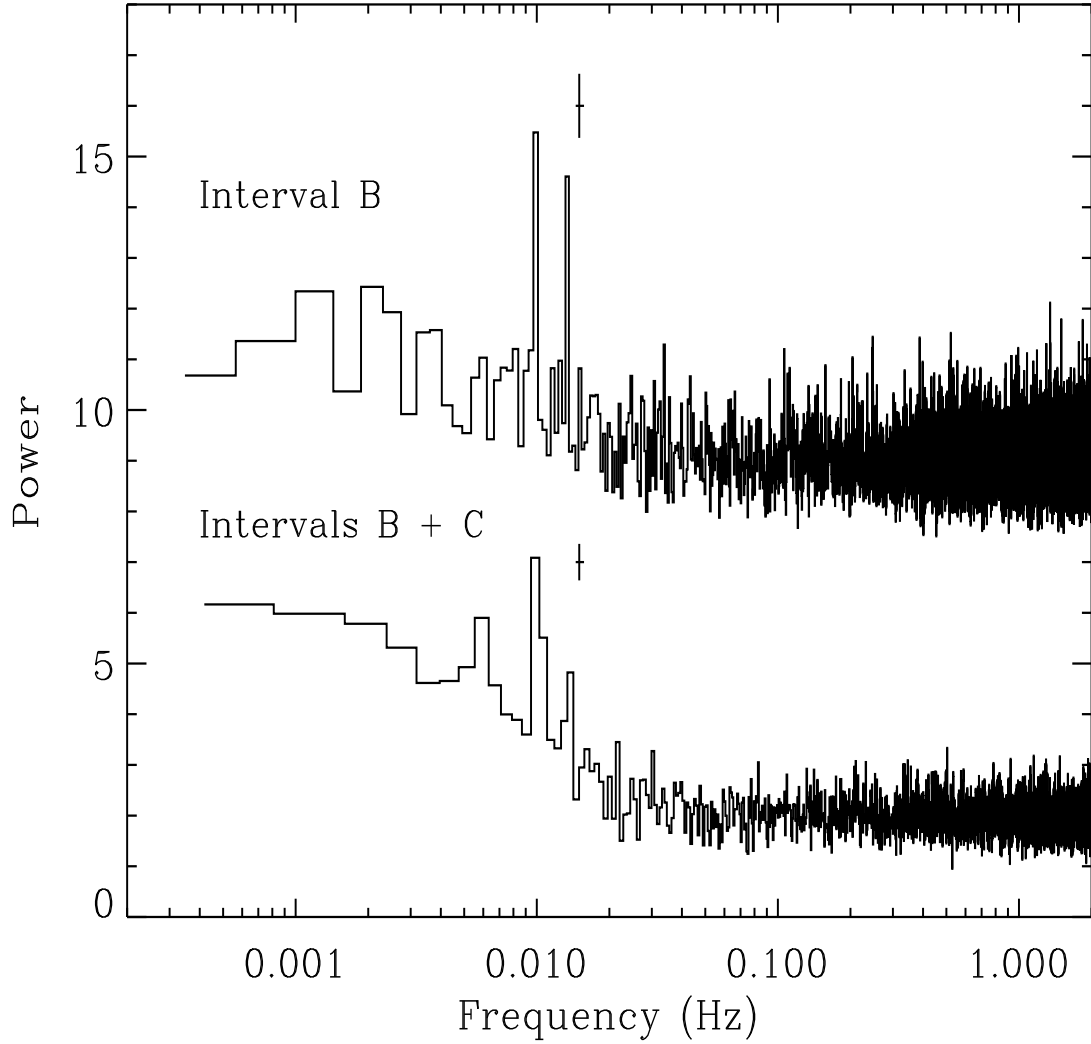


Figure 3: Average power spectrum of NGC 5408 X-1 from > 1 keV EPIC/pn data. The upper curve shows data from interval B with a frequency resolution of 0.434 mHz. Each bin is an average of 10 independent measurements. The bottom curve is an average of the two longest intervals (B and C) at a frequency resolution of 0.78 mHz. Each bin is an average of 32 independent measurements. See the text for additional discussion.

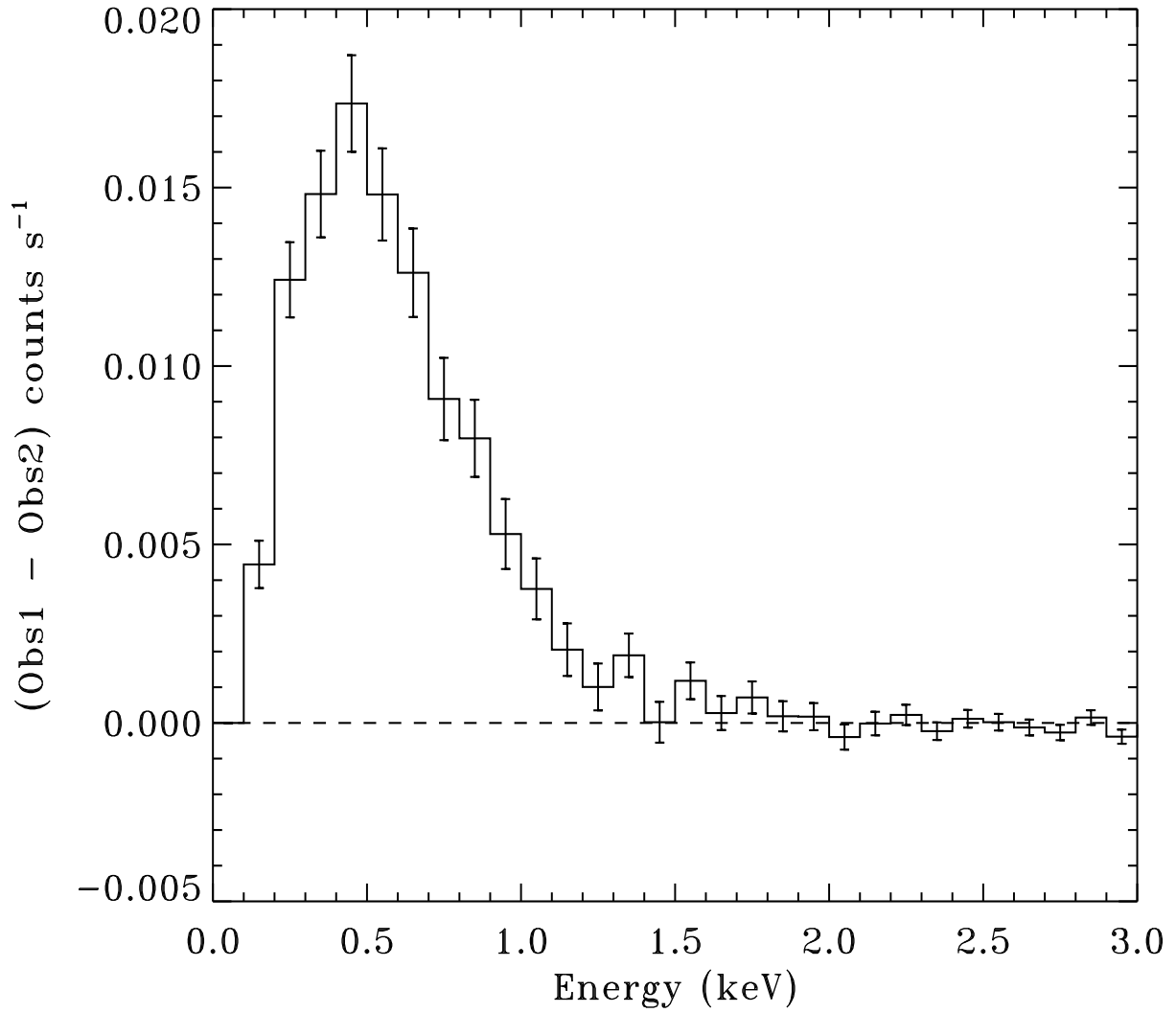


Figure 4: Difference of the count rate spectra between Observation 1 and Observation 2 (i.e. Obs1 - Obs 2). This shows that observation 1 was brighter, and that most of the difference was associated with < 1 keV photons, that is, the disk component.

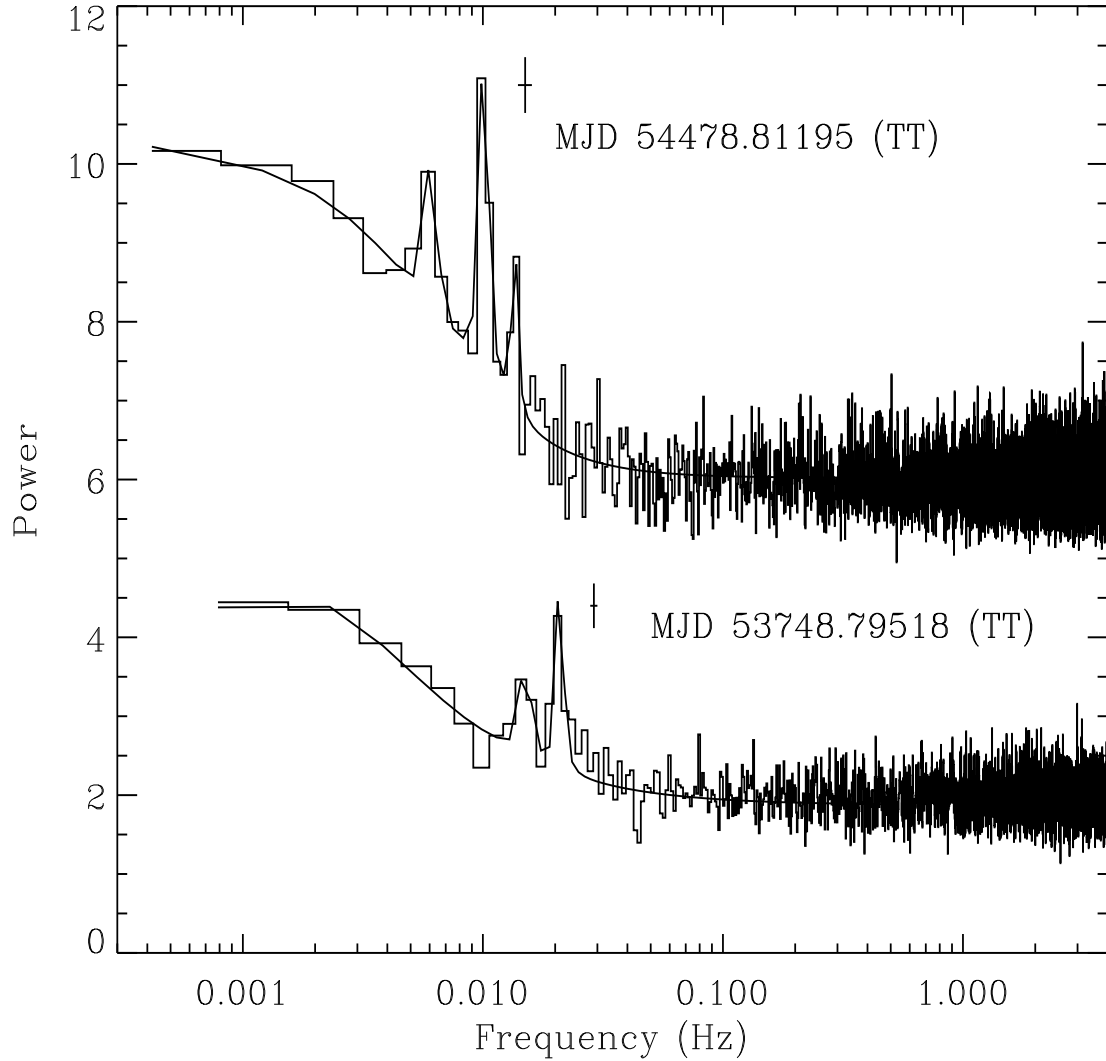


Figure 5: Average power spectra and best fitting models characteristic of both observations of NGC 5408 X-1 from EPIC/pn data. The upper curve is from the 2008 data (intervals B + C), while the bottom curve is from the 2006 data. See the text for additional details and Table 1 for a summary of the model parameters.

Table 1. Results of Power Spectral Modeling for NGC 5408 X-1¹

Parameters	2008, All intervals (Fig. 2)	2008, Interval B+C (Fig. 5)	2006 (Fig. 5)
A ^a	1.88 ± 0.2	3.4 ± 0.6	55.7 ± 5
α_L ^b	0.07 ± 0.08	0.029 ± 0.1	-0.42 ± 0.5
α_H ^c	1.83 ± 0.3	1.7 ± 0.4	1.2 ± 0.4
ν_{bend} (mHz) ^d	10.0 ± 3	6.3 ± 2	2.6 ± 2
r_{BB} (%) ^e	41 ± 5	45 ± 4	23 ± 4
ν_1 (mHz) ^f	10.02 ± 0.005	10.01 ± 0.002	20.6 ± 0.03
r_1 (%) ^g	17.4 ± 1.3	15.0 ± 1.2	8.4 ± 1.0
ν_2 (mHz)	NA	13.5 ± 0.1	15.1 ± 0.2
r_2 (%)	NA	10.0 ± 2	5.4 ± 1
ν_3 (mHz)	NA	6.0 ± 0.2	NA
r_3 (%)	NA	8.8 ± 2.5	NA
χ^2 (dof)	463 (459)	518.8 (497)	152.2 (180)

¹Summary of best fit power spectral models for NGC 5408 X-1. The results from fits to three different power spectra are shown in columns 2-4. Columns 2-4 show results using pn data, but for different time intervals. The particular time interval used is given with a reference in the heading to the figure the power spectrum appears in. These fits used up to three Lorentzian components, numbered 1-3 in order of increasing rms amplitude.

^aNormalization of the bending power-law component.

^bPower law index below the bend frequency.

^cPower law index above the bend frequency.

^dBend frequency, in mHz.

^erms amplitude of the broad-band continuum

^fCentroid frequency of the strongest QPO

^grms amplitude of the strongest QPO

^hCentroid frequency of the next strongest QPO

ⁱrms amplitude of the next strongest QPO

^jCentroid frequency of the weakest QPO

^krms amplitude of the weakest QPO

^lMinimum χ^2 of the fit

Table 2. Spectral Fits to XMM-Newton pn Spectra*

Spectral parameters	2006	2008
Model: <code>tbabs*(diskpn + apec + pow)</code>		
n_H^a	7.0 ± 0.5	6.5 ± 0.6
T_{max}^b	0.155 ± 0.004	0.160 ± 0.005
kT ^c	0.87 ± 0.05	0.85 ± 0.04
Γ^d	2.58 ± 0.04	2.47 ± 0.04
χ^2/dof	814/673	776/673
F_{disk} (0.3-10, keV) ^e	1.5×10^{-12}	1.1×10^{-12}
F_{pow} (0.3-10, keV) ^f	2.1×10^{-12}	1.9×10^{-12}
F_X (0.3-10 keV) ^g	3.7×10^{-12}	3.1×10^{-12}

^aHydrogen column density in units of 10^{20} cm^{-2} , not including the Galactic contribution of $n_{HGal} = 5.73 \times 10^{20} \text{ cm}^{-2}$.

^bDisk temperature in keV from the XSPEC disk model `diskpn`. The inner disk radius was fixed at $6 \text{ GM}/c^2$.

^cPlasma temperature in keV from the XSPEC model `apec`. The abundances were fixed to the solar values.

^dPower-law spectral index.

^eUnabsorbed flux from the `diskpn` component, in units of $\text{erg cm}^{-2} \text{ s}^{-1}$.

^fUnabsorbed flux from the power-law component, in units of $\text{erg cm}^{-2} \text{ s}^{-1}$.

^gUnabsorbed total flux in units of $\text{erg cm}^{-2} \text{ s}^{-1}$.

*All errors are quoted at the 90% confidence level.

Table 3. Mass Estimates for NGC 5408 X-1 from QPO Scaling*

Source	M_{dyn}^a M_{\odot}	ν_{qpo} range ^b Hz	$f_{min}, f_{best}, f_{max}^c$	$M_{min}, M_{best}, M_{max}^d$ M_{\odot}	Refs. ^e
XTE J1550–564	9.5 ± 1.1	2.5 - 6.5	125, 300, 650	1050, 2850 ± 330 , 6890	1, 2, 3
GRS 1915+105	14 ± 4	2.1 - 3.5	105, 185, 350	1050, 2590 ± 740 , 6300	2, 3, 4
H 1743–322	~ 11	3 - 5	150, 267, 500	1650, 2937, 5500	3, 5
XTE J1859+226	7.6 - 12.0	7.5	375, NA, 750	2850, NA, 9000	3, 6, 7
GX 339–4	> 6	5.9 - 7.8	295, 457, 780	1770, 2742, 4680	3, 8, 9
4U 1630–47 ^f	NA	4 - 8	200, 400, 800	NA	2

^aMass estimates for dynamically confirmed BHs.

^bRange of QPO frequencies observed when the spectral index ranges from 2.4 to 2.6.

^cScale factors derived from the observed QPO range. The “best” scale factor is derived by aligning to the center of the range. The minimum and maximum values are obtained by scaling the lowest observed frequency in the reference system with the highest observed frequency in NGC 5408 X-1, and vice versa. See §4 for discussion.

^dEstimated masses determined by scaling up the observed masses of the reference systems by the derived scale factors. The “best” mass estimate is obtained using the best scale factor, with uncertainties set by the uncertainties in the reference source masses. The minimum and maximum mass estimates are derived using the minimum and maximum scale factors and the $\pm 1\sigma$ mass limits. For example, the minimum mass for XTE J1550-564 is defined as $(9.5 - 1.1) * f_{min} = 8.4 \times 125 = 1050 M_{\odot}$. See §4 for additional discussion.

^eRelevant references for the mass and QPO frequency measurements: (1) Orosz et al. 2002; (2) Vignarca et al. 2003; (3) ST09; (4) Greiner, Cuby & McCaughrean 2001; (5) McClintock et al. 2009; (6) Fillipenko & Chornock 2001; (7) Zurita et al. 2002; (8) Munoz-Darias et al. 2008; (9) Hynes et al. 2004. measurements.

^fThere is no dynamical mass constraint for this source.